Dental Materials 40 (2024) 1591–1601

Contents lists available at ScienceDirect

Dental Materials

journal homepage: www.elsevier.com/locate/dental

Mitigating lipopolysaccharide-induced impairment in human dental pulp stem cells with tideglusib-doped nanoparticles: Enhancing osteogenic differentiation and mineralization

Raquel Osorio [a], Francisco J. Rodríguez-Lozano [b], Manuel Toledano [a,*], Manuel Toledano-Osorio [c], David García-Bernal [d], Laura Murcia [e], Sergio López-García [b]

[a] Faculty of Dentistry, University of Granada Colegio Máximo de Cartuja s/n, Granada 18071, Spain
[b] Department of Dermatology, Stomatology, Radiology and Physical Medicine, Morales Meseguer Hospital, Biomedical Research Institute (IMIB), Regional Campus of International Excellence "Campus Mare Nostrum", Faculty of Medicine, University of Murcia, Murcia 30008, Spain
[c] Postgraduate Program of Specialization in Periodontology, Faculty of Dentistry, University Complutense of Madrid, Madrid, Spain
[d] Department of Biochemistry, Molecular Biology B and Immunology, Faculty of Medicine, University of Murcia, Biomedical Research Institute (IMIB), Murcia 30120, Spain
[e] Department of Health Sciences, Catholic University San Antonio of Murcia, Murcia 30107, Spain

ARTICLE INFO

Keywords:
Cell proliferation
Tideglusib
Osteogenic differentiation
Stem cells
LPS

ABSTRACT

Objective: Drug-loaded non-resorbable polymeric nanoparticles (NPs) are proposed as an adjunctive treatment for pulp regenerative strategies. The present in vitro investigation aimed to evaluate the effectiveness of tideglusib-doped nanoparticles (TDg-NPs) in mitigating the adverse effects of bacterial lipopolysaccharide endotoxin (LPS) on the viability, morphology, migration, differentiation and mineralization potential of human dental pulp stem cells (hDPSCs).

Methods: Cell viability, proliferation, and differentiation were assessed using a MTT assay, cell migration evaluation, cell cytoskeleton staining analysis, Alizarin Red S staining and expression of the odontogenic related genes by a real-time quantitative polymerase chain reaction (RT-qPCR) were also performed. Cells were tested both with and without stimulation with LPS at various time points. One-way ANOVA and Tukey's test were employed for statistical analysis ($p < 0.05$).

Results: Adequate cell viability was encountered in all groups and at every tested time point (24, 48, 72 and 168 h), without differences among the groups ($p > 0.05$). The analysis of cell cytoskeleton showed nuclear alteration in cultures with undoped NPs after LPS stimulation. These cells exhibited an in blue diffuse and multifocal appearance. Some nuclei looked fragmented and condensed. hDPSCs after LPS stimulation but in the presence of TDg-NPs exhibited less nuclei changes. LPS induced down-regulation of Alkaline phosphatase, Osteonectin and Collagen1 gene markers, after 21d. LPS half-reduced the cells production of calcium deposits in all groups ($p < 0.05$), except in the group with TDg-NPs (decrease about 10 %).

Significance: LPS induced lower mineral deposition and cytoskeletal disorganization in hDPSCs. These effects were counteracted by TDg-NPs, enhancing osteogenic differentiation and mineralization.

1. Introduction

Pulp inflammation occurs if superficial caries are not treated in time. Bacteria or bacterial by-product remain present in the dentin where they cause chronic inflammation, leading to reparative events [1]. Bacterial lipopolysaccharide endotoxin (LPS) is commonly detected in infected pulp cavities and root canals. As well as being an important etiologic factor for pulpitis and apical periodontitis [2]. LPS is also postulated to have profound effects on proinflammatory cytokine production [3]. LPS facilitates the release of inflammatory cytokines such as tumor necrosis factor-alpha (TNF-α) interleukin 1 beta (IL-1β), interleukin 6 (IL-6), IL-8 and IL-10 [4,5].

In some cases, direct pulp capping is indicated for treating dental pulp exposure by using biomaterials to stimulate the reparative

* Correspondence to: Faculty of Dentistry, University of Granada, Granada, Spain.
E-mail address: toledano@ugr.es (M. Toledano).

https://doi.org/10.1016/j.dental.2024.07.012
Received 17 June 2024; Received in revised form 18 July 2024; Accepted 23 July 2024
Available online 26 July 2024

formation and enhance the remineralization of the existing dentin [6]. Traditional sealing cements on dentin have been used to stimulate remineralization, but these agents do not form a biological union with tooth structure and can cause weakening of the histologic substrate [7] with, normally, little presence of reparative cells. In response to tissue injury, mesenchymal stem cells proliferate and migrate to the injured area, where they differentiate toward an odontogenic phenotype showing both osteogenic and odontogenic profiles [6] to deposit reparative hard tissue [8]. It has been shown that dentinogenesis shares multiple properties with intramembranous bone formation [9].

Wnt signaling is a signaling pathway that participates in reparative hard tissues formation [10]. Activating Wnt signaling via a small-molecule Wnt agonist that provides both stability and suitability for clinical use could be a promising strategy for hard tissues repair [6]. Glycogen synthase kinase 3β (GSK-3β) is a serine/threonine protein kinase that plays a central role in the regulating Wnt/β-catenin signaling pathway [11]. Phosphorilated GSK-3β degrades β-catenin in the absence of Wnt-receptor interaction. Active β-catenin interacts with Tcf/Lef transcription factor and up-regulates gene expression involved in cell differentiation [7]. Small molecules stimulate the signal transduction, speed up the natural healing process, can mimic growth factors, trigger a controlling point of cellular signal transduction system, and act altering gene expression [7]. Tideglusib (TDg) is one of the small molecules that activate canonical Wnt signaling by inhibiting the GSK-3β activity [12]. TDg is a commercially available medication developed for treating progressive supranuclear palsy and Alzheimer's disease [13]. TDg has increased osteoblastogenesis, has promoted anabolic effects on bone formation, and it has enhanced reparative dentin and mature mineral formation under the injury site [6,14].

However, for TDg to be used clinically, a controlled and sustained release delivery system would be necessary to induce odontoblast and osteoblast differentiation. Various delivery vehicles can be used to provide sustained drug release and tissue guidance. Many natural and synthetic polymers are being used as delivery vehicle in the form of different scaffolds such as nanofibers, membranes, gels, microspheres and nanoparticles (NPs) [7]. Polymeric NPs generated by polymerization/precipitation may be loaded with TDg [14,15].

It was the objective of this in vitro investigation to evaluate the effectiveness of tideglusib-doped nanoparticles (TDg-NPs) in mitigating the adverse effects of lipopolysaccharide (LPS) in terms of cell viability, migration, gene expression, cell morphology or mineralization on human dental pulp stem cells (hDPSCs). The null hypothesis was that there are no differences among the different cultures in term of viability, wound healing, morphology of the cytoskeleton, odontogenic markers expression and calcification ability of hDPSCs cultured in the presence of TDg-NPs, with or without LPS.

2. Materials and methods

2.1. Production of nanoparticles

The process of obtaining NPs applied the use of the polymerization precipitation method, which controlled the precipitation facilitated by a thermodynamic approach. Specifically, the Flory-Huggins model, based on Hansen's solubility parameters, was employed. This model centered on interactions among solvent molecules and the growth of polymer chains through hydrogen, polar bonding, and dispersion forces [16]. The backbone monomer for NP design was 2-hydroxyethyl methacrylate, with methacrylic acid serving as the functional monomer, and ethylene glycol dimethacrylate employed as the cross-linker. Subsequently, half of the produced NPs were loaded with a peptide, TDg (Sigma-Aldrich, Chemie GmbH, Riedstr, Germany). The NPs loading process was conducted by immersion of 100 mg of NPs in 1 mL of 0.0017 mg/mL TDg solution for 2 h at room temperature under constant shaking (12 rpm) (rotator Orbit 300445, JP Selecta, Barcelona, Spain). Then, the NPs were left until the solvent was completely evaporated, ensuring that all the TDg remains onto the NPs. Two types of NPs were obtained, undoped NPs and TDg-NPs.

2.2. Cell harvest, isolation and characterization

Mesenchymal stem cells were obtained from impacted third molars (n = 10), which were extracted from 10 healthy subjects aged between 18 to 30 years. The protocol for human dental pulp cells (hDPCs) isolation was approved by the Human Research Ethics Committee from the University of Murcia (protocol ID: 457/2023). It followed the guidelines from the Declaration of Helsinki. In order to generate single cell suspensions, the pulp was gently removed, and then washed with Ca/Mg-free Hank's balanced salt solution (Gibco Invitrogen, Paisley, Scotland), and after incubated in the presence of collagenase A (3 mg/mL) (Sigma-Aldrich, St Louis, MO), for 1 h at 37 °C. Cells then were seeded onto plastic tissue culture flasks (BD Biosciences, San Diego, CA) immersed in Dulbecco modified Eagle medium (DMEM; Gibco Invitrogen, Paisley, Scotland), which was supplemented with penicillin/streptomycin (PAA Laboratories, Pasching, Austria), L-glutamine (PAA Laboratories), and 10 % fetal bovine serum (FBS) (Gibco Invitrogen) and incubated for 3 d, at 37 °C in a humid atmosphere containing 7.5 % CO_2. After adherent cells were visualized erythrocytes and non-adherent cells were removed trough washing with Ca/Mg-free phosphate-buffered saline (PBS) (Gibco Invitrogen). After cultures reached 80 % of confluence, cells were newly washed with PBS and detached with 0.25 % trypsin EDTA solution (Gibco Invitrogen) for 3–5 min, at 37 °C. Cells were then seeded at a density of 6×10^3 cells/cm^2 until reaching 80 % to 90 % of cell confluence. To reduce the impact of interindividual heterogeneity in MSCs from donors, pooled hDPSC samples from 5 to 8 different donors were used in various experiments [17].

Human DPSCs were immunophenotyped by flow cytometry using specific antibodies for mesenchymal markers (CD73, CD90, CD105) and hematopoietic markers (CD14, CD20, CD34, CD45) with the human MSC phenotyping cocktail from Miltenyi Biotec (Bergisch Gladbach, Germany) on a FACS LSR Fortessa flow cytometer (Becton Dickinson, Franklin Lakes, NJ, USA). Each experiment was performed in triplicate.

For half of the groups, cells were incubated in the presence of *E. coli* LPS (1 μg/mL) (Sigma-Aldrich/Merck) [18]. 24 h after cell seeding, when the cells spread and reached the appropriate confluence, LPS and/or NPs were added. From this point, fresh cell medium with or without LPS was replaced every two days until the time of each specific experiment.

2.3. Analysis of hDPSC proliferation

The proliferation of the hDPSCs of the different groups was quantitatively assessed with a MTT (3-(4,5-dimethylthiazol-2-yl)−2,5-diphenyltetrazolium bromide) assay (MTT Cell Growth Kit; Chemicon, Rosemont, IL). It measures the cellular metabolic activity, as an indicator of cell viability and proliferation. This assay determines the mitochondrial dehydrogenase enzymes ability to convert the yellow water-soluble tetrazolium salt MTT into the colored compounds of formazan. The measured absorbance of formazan is therefore proportional to the amount of living cells. Proliferation of hDPSCs was analyzed after at 24, 48, 72 and 168 h of culture and treatment with different concentrations of NPs. For that purpose, wells were washed twice with PBS, and then 50 mL MTT solution (1 mg/mL) was added to the culture and incubated for 4 h. Each well was washed with 300 mL of PBS, 100 mL of dimethyl sulfoxide were added to extract and solubilize the formazan. Absorbance at 570 nm was then measured by using an automatic microplate reader (ELx800; Bio-Tek Instruments, Winooski, VT) using an absorbance of 690 nm as the reference wavelength value. Each experimental condition was analyzed in quintuplicate [17].

2.4. Cell migration evaluation (scratch wound assay)

A horizontal scratch wound healing assay was carried out to assess the migration ability of hDPSCs in response to the several NPs. The hDPSCs were seeded at a concentration of 2×10^5 cells in a 12-well plate. Thereafter, a 200 μL pipette tip was used to scratch through the confluent layer of cells and they were exposed to the diverse groups of study. Wound closure was analyzed at three time intervals: 0–24 h (first time interval), 24–48 h (second time interval), and 48–72 h (third time interval). Phase-contrast microscopy (Olympus, Japan) was used to take images of the wound area after scratching. Twelve acquired images per group were used for analysis by *ImageJ* v. 1.53e software (National Institutes of Health, Bethesda, MD, USA). To account for the width variations among the scratch wounds, migration rates were presented as percentage areas of relative wound closure (RWC) and calculated as RWC (%) = (wound closure area in pixels/total number of pixels) × 100 [19].

2.5. Cell morphology and spreading

Cell morphology and spreading were assessed by fluorescent-phalloidin labeling. A density of 3×10^4 cells was seeded in a 24-well plate, allowed to adhere, spread, and cultured in untreated medium (control) or NPs for 72 h at 37°C. Then, 1 mL of 4 % paraformaldehyde (PFA) solution was added to each sample for 15 min at room temperature to fix the hDPSCs on the surface. They were then permeabilized with 1 mL of Triton X-100 (Solarbio, Beijing, China). The cells were then gently rinsed with phosphatebuffered saline (PBS) twice. The hDPSCs were stained successively with 4,6-diamidino2-phenylindole dihydrochloride (DAPI) (ThermoFisher Scientific, Waltham, MA, USA) and Invitrogen™ AlexaFluor™594-labeled phalloidin (ThermoFisher Scientific), at r/t in the dark for 30 min [19]. Fluorescence images were acquired with a Nikon N-STORM confocal microscope (Nikon Corporation, Tokyo Metropolis, Japan) using NIS-Elements Viewer Software (Nikon Corporation, Tokyo Metropolis, Japan).

2.6. Cell odontogenic gene expression: RT-qPCR assay

To determine mRNA transcript levels of the odontogenic differentiation and mineralization markers, the hDPSCs were cultured together with the tested NPs. A real-time quantitative polymerase chain reaction (RT-qPCR) was performed to quantify gene expression. Twenty thousand hDPSCs per well were seeded onto 12-well plates (n = 3) and incubated for 7 and 21 d with 10 μg/mL NPs-conditioned medium, in unconditioned culture medium (negative control group), or in osteogenic differentiation medium (*OsteoDiff*® media; Miltenyi Biotec, Gladbach, Germany) (positive control group). Culture media and eluates were replaced every three days. Total RNA from each culture was extracted using the RNeasy Mini Kit (Qiagen, Hilden, Germany) according to the manufacturer's protocol. 1 μg of RNA was reverse transcribed for first-strand complementary DNA (cDNA) synthesis via iScript™ Reverse Transcription Supermix for RT-qPCR (Bio-Rad Laboratories Inc., Hercules, CA, USA) [19,20].

The sequences of relevant primers were as follows: (5^0-3^0): alkaline phosphatase or *ALP* (forward: TCAGAAGCTCAACACCAACG, reverse: TTGTACGTCTTGGAGAGGGC), osteonectin or *ON* (forward: CGGGTGAAGAAGATCCATGAG, reverse: CTGCCAGTGTACAGGGAAGATG), collagen type 1 or *Col1A1* (forward: CTAAAGGCGAACCTGGTGAT, reverse: TCCAGGAGCACCAACATTAC), runt-related transcription factor 2 or *RUNX2* (forward: TCCACACCATTAGGGACCATC, reverse: TGCTAATGCTTCGTGTTTCCA), bone sialoprotein or *BSP* (forward: TGCCTTGAGCCTGCTTCCT, reverse: CTGAGCAAAATTAAAGCAGTCTTCA), amelogenin X or *AMELX* (forward: CACCCTGCAGCCTCATCACC, reverse: GTGTTGGATTGGAGTCATGG), Ameloblastin or *AMBN* (forward: AGCCATGTTTCCAGGATTTG, reverse: TGCACCTCCTTCTTCGTTCT). Differentiation markers were measured using the expression of the housekeeping gene Glyceraldehyde 3-phosphate dehydrogenase (*GAPDH*) as a reference, with the following sequence (5^0-3^0): (forward: TCAGCAATGCCTCCTGCAC, reverse: TCTGGGTGGCAGTGATGG). To calculate the relative gene expression, the standardized $2^{-\Delta\Delta CT}$ method was used [20].

2.7. Cell mineralization/calcified nodule formation: Alizarin Red S Staining

The mineralization or calcification ability of the hDPSCs in contact with the tested NPs was analyzed by Alizarin Red S Staining (ARS) after 21 d of culture. The hDPSCs were seeded onto 24-well plates at 1×10^4 cells/well concentrations and allowed for attachment. The cells were then transferred into the NPs-conditioned medium and cultured for 21 d. After the culture period, the cells were fixed in 95 % ethanol for 30 min at room temperature (RT), rinsed three times with double-distilled water, stained with 5 % of alizarin red (pH = 4.2, Sigma Aldrich, St. Louis, MO, USA) for 5–10 min, washed repeatedly with double distilled water, and then dried at RT. The dried plate was observed under a stereomicroscope (Leica Microsystems GmbH, Wetzlar, Germany) to acquire relevant images. For quantification of the calcified nodules, the alizarin red was dissolved in 10 % cetylpyridinium chloride (Sigma-Aldrich, MO, USA). After that, the plate was read at an absorbance of 405 nm by the spectrophotometric microplate reader (Thermo Fisher, USA) [19]. For this assay, both a negative control (hBMMSCs cultured in unconditioned growth medium, DMEM; Gibco, USA) and a positive control (hBMMSCs cultured in osteoinductive media (*OsteoDiff*®, Miltenyi Biotec, Germany) were used for reference.

2.8. Statistical Analysis

Statistical analyses were performed with Prism 6 (GraphPad Software, San Diego, CA, USA). Data are expressed as mean ± standard deviations (SD). The normality in the distribution of the data was previously confirmed via a Q-Q plot. Data were analyzed using one-way ANOVA and Tukey's post hoc test. Statistical significance was set at $p < 0.05$.

A flowchart of the whole methodology is presented at Fig. 1.

3. Results

3.1. Cell characterization

hDPSCs exhibit numerous phenotypic characteristics in vitro that are commonly associated with bone marrow-derived mesenchymal stem cells (MSCs). To identify specific cell surface molecules, flow cytometric analysis was employed. The analysis revealed that hDPSCs display the characteristic pattern of MSC-associated surface markers, including CD73, CD90, and CD105. Additionally, hDPSCs were negative for hematopoietic stem cell surface markers such as CD14, CD20, CD34, and CD45 (Fig. 2).

3.2. MTT assay

To investigate the effects of varying concentrations of different NPs on the proliferation rates of hDPSCs, an MTT assay was performed. Adequate cell viability was encountered in all cases and at every tested time point (24, 48, 72 and 168 h), without significant differences among the tested experimental groups ($p > 0.05$) (Fig. 3).

3.3. Wound healing assay

Cell monolayers were wounded by a scraper and allowed to heal under various conditions. The cells cultured showed similar behavior to that of the untreated group (control) at every time in the wound healing assay ($p > 0.05$). Differences between the several tested periods of time

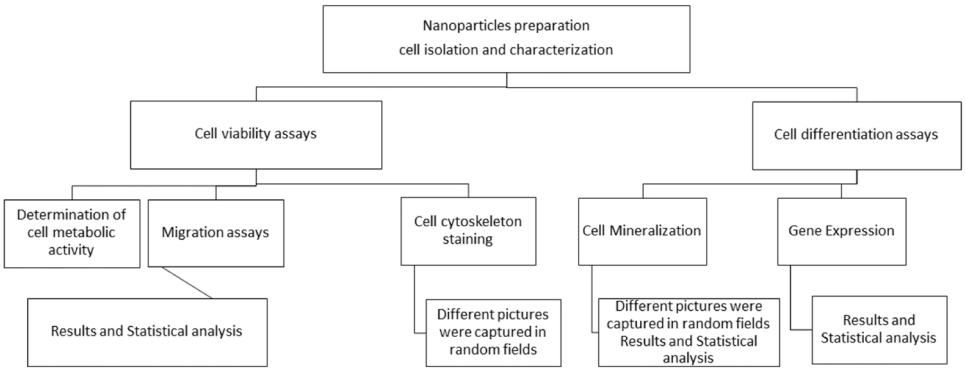

Fig. 1. Flowchart reflecting the methodology that was followed to undertake the present research.

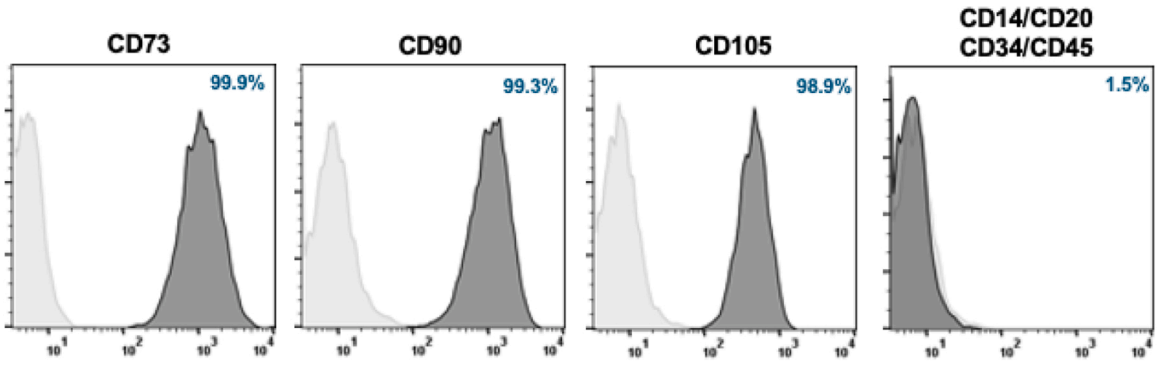

Fig. 2. Histograms from the hDPSCs phenotyping performed by flow cytometry using specific antibodies for the mesenchymal surface markers CD73, CD90, CD105, and the haematopoietic markers CD14, CD20, CD34, CD45 (dark grey histograms). The numbers inside the histograms indicate the percentage of positive cells for each marker compared to isotype antibody staining (light grey histograms).

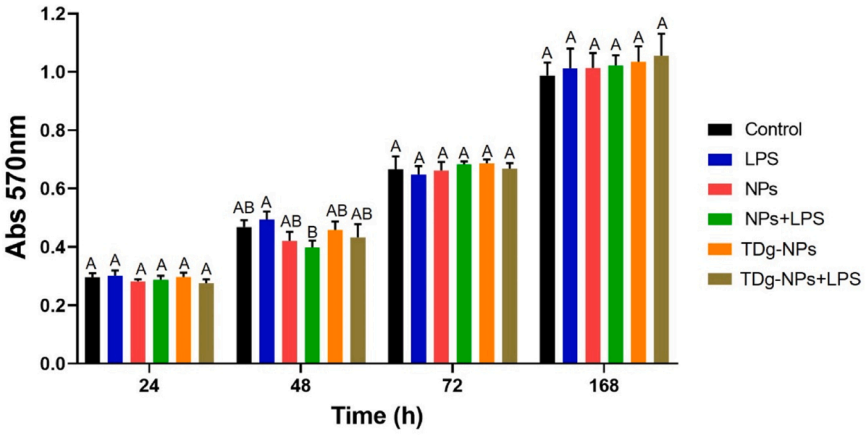

Fig. 3. MTT assay results. The hDPSCs viability was analyzed at 24, 48, 72 and 168 h of culture in the presence of NPs and in the control groups. Fluorescence intensity was assessed using spectrophotometry at 570 nm. Each experiment was performed in triplicate. No differences were found among the experimental groups ($p > 0.05$).

(24, 48 and 72 h) were always significant ($p < 0.05$), corresponding higher healing rates to the longer time periods (Fig. 4).

3.4. Cell cytoskeleton labeling

Cell adhesion and morphology were investigated by staining hDPSCs with phalloidin (red fluorescence) and DAPI (blue fluorescence) to visualize the actin cytoskeleton and cell nuclei, respectively. Immunofluorescence staining evidenced that the cells treated with the tested NPs exhibited a mesenchymal/fibroblastic cell morphology, similar to the control group. The cells exhibited substantial extension, and overall, the cell morphology varied significantly between groups with and without LPS exposure. This variation was characterized by distinct distributions of actin filaments and organelles along cytoskeletal cables and patches, as evidenced by the regular display of F-actin. In cultures exposed to LPS, some cells appeared poorly organized and partially disrupted, exhibiting aberrant morphology. In presence of TDg, even with LPS, cultured cells were flattened and wide-spread cell body with a structured cytoskeleton. Some nuclear alterations were also detected in the groups of *OsteoDiff*®+LPS and NPs+LPS. Remarkably, nuclear changes were

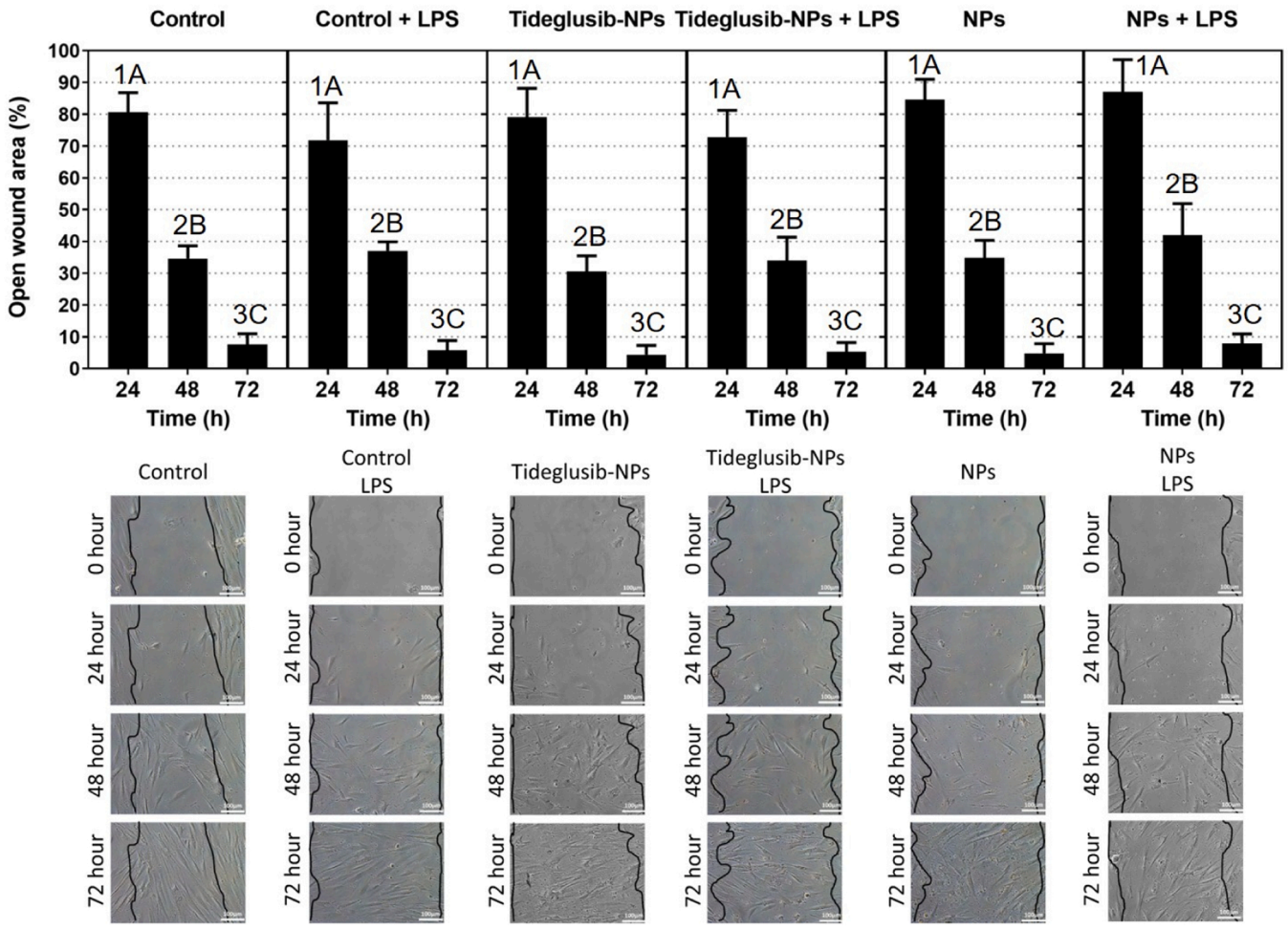

Fig. 4. Mean and standard deviations of the different calculated wound-healing rates in the experimental groups. Representative optical microscope images of the hDPSCs migration in the presence of the different NPs and in the control group are shown. The scale bar is 100 μm. Statistical analysis corresponds to the wound-healing rate. Similar letters, within each group, indicate no significant differences ($p > 0.05$). Similar numbers, among groups, indicate no significant differences ($p > 0.05$).

less adverted in the group of TDg-NPs+LPS. The cells mainly displayed an elongated and spread morphology, with evident similarities to the cells cultured in the control groups (Fig. 5).

3.5. RT-qPCR assay

The results of the RT-qPCR assay for assessing odontogenic/osteogenic marker expression from the hDPSCs cultured with the tested NPs (10 μg/mL) are presented in Fig. 6. The RT-qPCR assays evidenced a marked overexpression of ALP gene at 3 d, in *OsteoDiff*® media, significantly higher than that obtained for the rest of the groups, which performed similar ($p < 0.001$). At 21 d time point, *ALP* was down-regulated in *OsteoDiff*® media and in all groups containing LPS (*OsteoDiff*®+LPS, NPs+LPS, TDg-NPs+LPS) ($p < 0.001$). Concerning *DSPP*, untreated cells (control) showed the highest expression at 3 d time point. At 3 d evaluation, the presence of TDg down-regulated the gene expression of *DSPP*. At 21 d, the control group exhibited the lowest *DSPP* expression, while the *OsteoDiff*® group showed the highest *DSPP* gene expression. The remaining groups exhibited intermediate levels of *DSPP* gene expression at the 21d time point ($p < 0.001$). Regarding *RUNX2*, the cells in the *OsteoDiff*® group attained significant overexpression ($p < 0.001$) at both time points (3 and 21 d). At 3 d, the presence of TDg in the NPs down-regulated the gene expression of *RUNX2*. At 21 d, disregarding the control group, the cells with undoped NPs attained the highest gene expression of *RUNX2*, and those with TDg-NPs in the presence of LPS, the lowest expression ($p < 0.001$). Concerning *COL1A1*, the cells cultured with *OsteoDiff*® media with or without LPS achieved the highest *COL1A1* expression, at 3 d time point. Cells cultured in unconditioned medium (control) and LPS-NPs evidenced the lowest *COL1A1* expression. Interestingly, at 21 d time point, two groups were clearly differentiated: cells cultured with *OsteoDiff*® media, with undoped NPs and with TDg-NPs that showed the highest *COL1A1* gene expression, and the rest of the groups showed a lower expression ($p < 0.001$). Cells cultured with *OsteoDiff*® media, at 3 d time point overexpressed *ON* in comparison with the rest of the groups. At 21 d, both *OsteoDiff*® media and undoped NPs facilitated the highest gene expression of *ON* among groups ($p < 0.001$). Concerning *BSP*, cells cultured both 3 and 21 d showed the same gene expression, except the cells cultured in the control group and assessed at 21 d, that down-regulated in comparison with the rest of the groups ($p < 0.001$). The cells cultured in the control group expressed the highest values of *AMLX*, at 3 d time point. The lowest values corresponded to the groups with TDg. At 21 d, the control group (negative control) showed the lowest gene expression of *AMLX*, and *OsteoDiff*® media the highest expression ($p < 0.001$).

3.6. Alizarin Red S Staining (ARS)

After 21 d of culturing, the groups in the presence of NPs and controls, were subjected to ARS staining to ascertain the cells' calcification

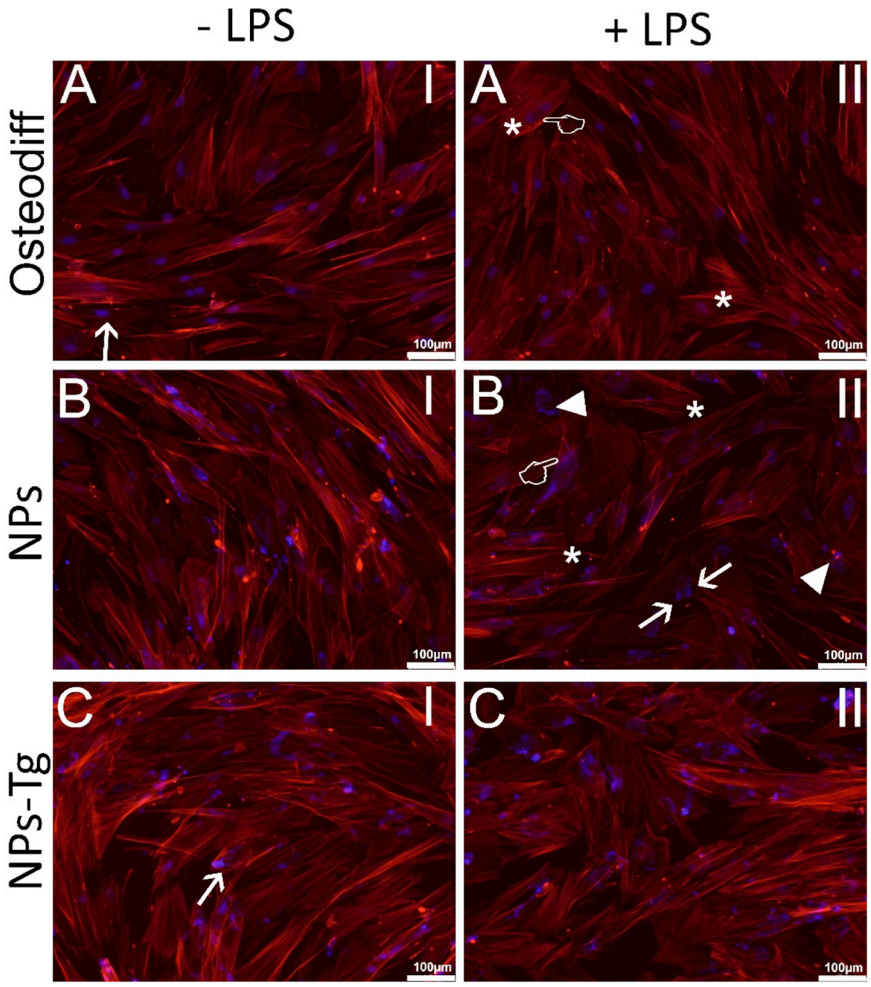

Fig. 5. Confocal microscopy images of the cytoskeletal component distribution after AlexaFluor™ 594-labeled phalloidin and DAPI staining F-actin fibers and nucleus, respectively, cultured in *OsteoDiff*® (**A**), NPs (**B**) and TDg-NPs (**C**). In general, hDPSCs showed typical long spindle shape, cytoskeleton could be observed showing a high F-actin content, and the round nucleus was located in the center of the cells when they were cultured without LPS (5 A·I, 5B·I, 5 C·I) (arrows). Some nuclei alterations were encountered in the hDPSCs cultured with *OsteoDiff*® and NPs, in presence of LPS (4 A·II, 4B·II). These cells showed an in blue diffuse (pointers) and multifocal (arrowheads) appearance. Some nuclei appeared fragmented and condensed (faced arrows). Cells cultured with TDg-NPs and LPS showed a lower amount of nuclei changes. In the rest of the experimental groups, there were no apparent deviation from normality, regarding the nuclear and cellular morphology, though the presence of LPS in the culture was associated to disorganization of microfilaments (asterisks). (4 A·II, 4B·II, 4 C·II). Blue fluorescence indicates cell nuclei; red fluorescence indicates the actin cytoskeleton. The scale bar is 100 µm.

ability (Fig. 7). hDPSCs cultured with *OsteoDiff*® media showed higher extensive clusters of calcium deposits than the rest of the groups. The presence of LPS significantly reduces calcium deposits by approximately 50 % in all cultured cell groups ($p < 0.001$). Notably, the inclusion of TDg effectively counteracts this decrease, restoring calcium deposition levels.

4. Discussion

In this study, we hypothesized that the biological effects of LPS on human dental pulp stem cells (hDPSCs) are mitigated by the presence of Tideglusib-doped nanoparticles (NPs). Cell groups cultured in the presence of LPS showed reduced calcium deposits and altered actin cytoskeleton organization compared to cultures without LPS. Cell cultures containing both LPS and TDg-NPs were less affected, demonstrating greater mineralization and more advanced actin cytoskeleton reorganization compared to the other cell groups exposed to LPS (Figs. 5 and 7). Thereby, the results of the present research partially support the rejection of the null hypothesis.

Our results demonstrated that hDPSCs exhibited reduced mineralization in the presence of LPS. When bacteria components or biofilm are present, they interfere with odontoblasts-like cell differentiation and mineralization of dental stem cells [1]. Thus, Vaseenon *et al.* (2023) [4] have previously reported that 20 µg/mL of LPS have interfered with mineralization, as mineralized nodule formation and gene expression of osteo/odontogenic differentiation were significantly decreased. Similarly, Rothermund *et al.* (2022) [8] determined that LPS reduced the capacity of DPSCs to mineralize the extracellular matrix, indicating that LPS inhibits terminal differentiation of DPSCs toward an odontoblastic phenotype. Hence, it can be clearly established that the presence of LPS induces functional differences in mineral deposition. This phenomenon may be attributed to elevated levels of β-catenin signaling in an inflammatory microenvironment [18], which may attenuate the noncanonical Wnt/calcium signaling pathway, thereby down-regulating the osteogenic differentiation capacity of stem cells [18,21]. Moreover, TDg as an anti-inflammatory compound [22] is related to the inhibition of NF-κB pathway. Therefore, in LPS stimulated cells, TDg reduces the expression of IL-1β, IL-6 and IL-8 and up-regulates odontoblastic markers, facilitating mineralization [5].

The osteogenic differentiation medium (*OsteoDiff*®) that was used as positive control in the present study, reduces the expression level of β-catenin but induces the activation of Ca^{2+}/calmodulin-dependent

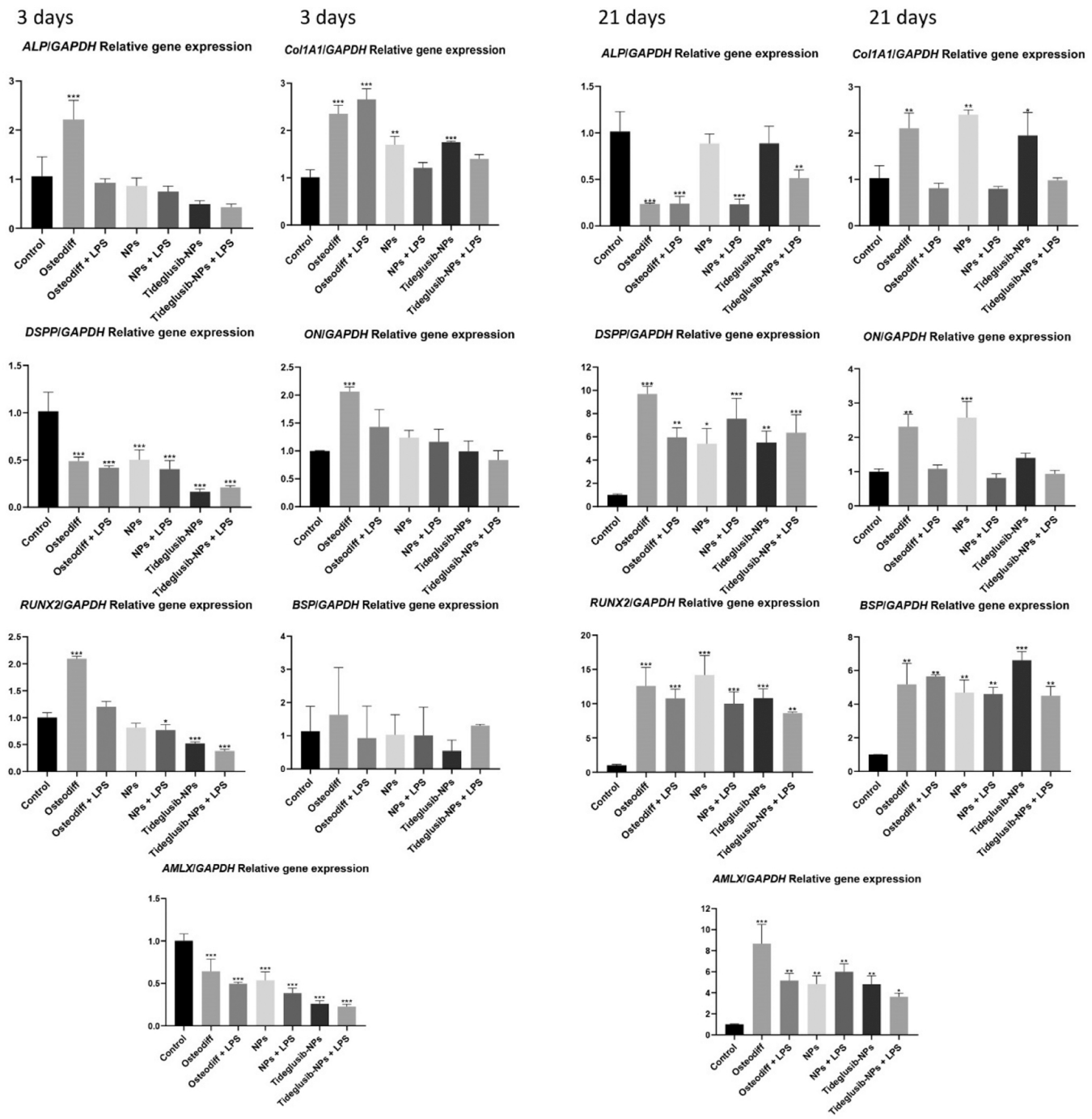

Fig. 6. Mean and standard deviations of the relative mRNA expressions from the selected osteogenic and odontogenic related genes: alkaline phosphatase (*ALP*), dentin sialoprotein (*DSPP*), *RUNX-2*, collagen A type 1 (*COL1A1*), osteonectin (*ON*), bone sialoprotein (*BSP*) and amelogenin (*AMELX*). The genes' cell expression was determined by RT-qPCR after osteogenic induction in the hDPSCs cultured for 3 and 21 d in the presence *OsteoDiff* ® media (positive control) with or without LPS, NPs with or without LPS, and TDg-NPs with or without LPS. Similar letters indicate no significant differences ($p < 0.05$).

protein kinase II (CaMKII), which in turn stimulates nemo-like kinase (NLK), resulting both in enhanced osteogenic differentiation and in the highest mineralization attained in the present study (Fig. 7). In all cases LPS produced a half-reduction in the mineralization ability of cultured cells, except in the presence of TDg NPs where the reduction was lower than 20 % (Fig. 7). Therefore, in the presence of LPS, TDg enhances the reparative or regenerative mineralization of hDPSCs. Tabassum *et al.* (2023) [7] have shown an interaction of TDg with GSK-3β, that performs as Wnt signaling antagonist. This interaction can inhibit the activity of GSK-3β and increase the stabilization of *β*-catenin, obtaining mineralization at 14 d. This outcome demonstrated that Wnt activation by TDg may facilitate hDPSC osteogenic differentiation in inflammatory microenvironments. As it has been previously reported that activation of canonical Wnt signaling at the injured dental pulp is involved in the process of dentin bridge formation, and it promotes the healing of the dentin-pulp complex [23,24]. Therefore, the clinical application of TDg-NPs as a dental pulp capping material that will activate the canonical Wnt signaling may be a new conservative an efficient dental pulp therapy [25].

Osteoblastic differentiation of the hDPSCs has been assessed by

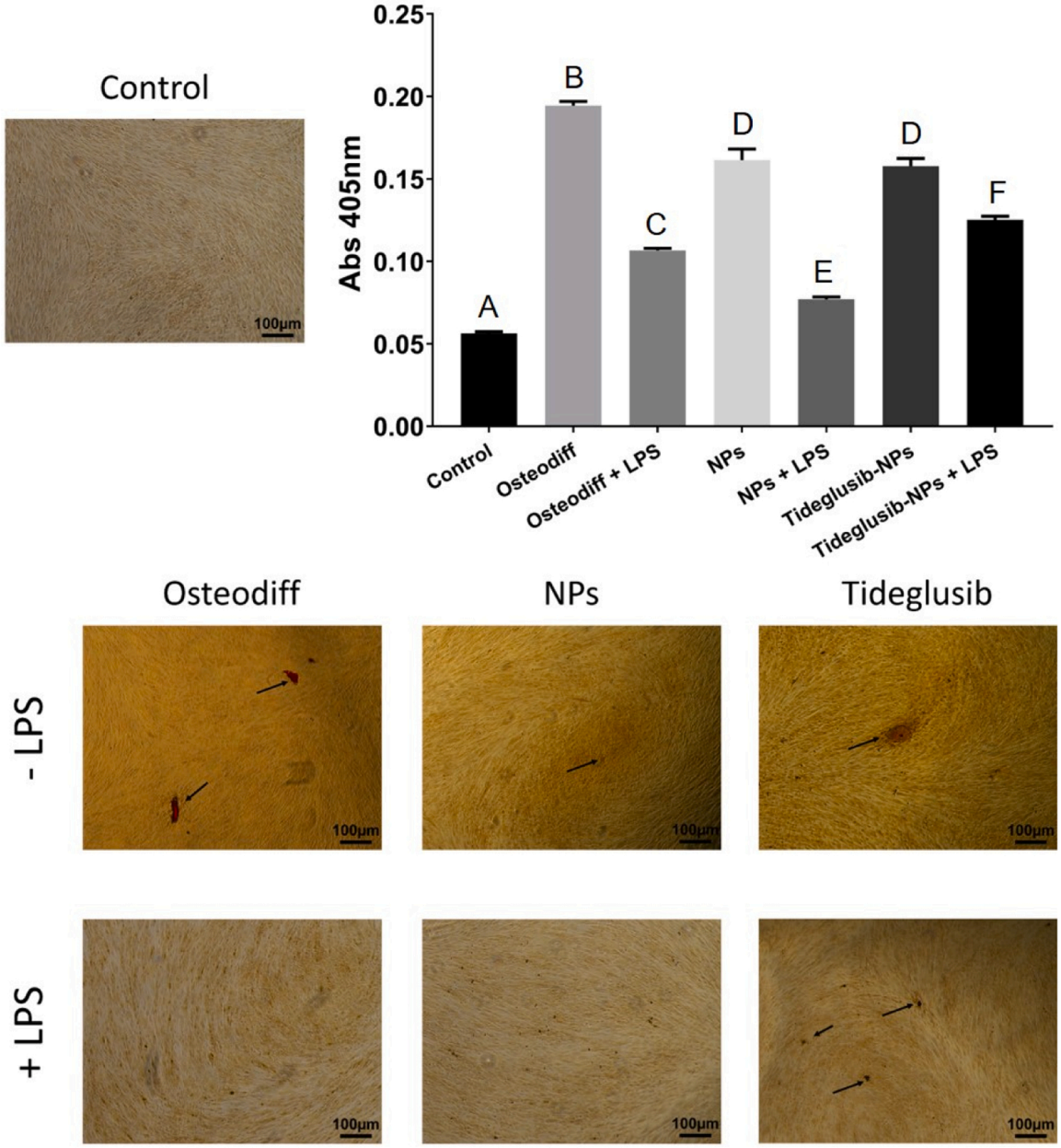

Fig. 7. Assessment of hDPSCs calcification ability with ARS after 21 d in the presence of the experimental NPs and in the control groups. Some calcium deposits are visible (black arrows). The mean and standard deviations of ARS were measured by the spectrophotometric microplate reader. Representative optical images of the ARS-stained areas in the different experimental groups are presented. Similar letters indicate no significant differences ($p < 0.05$).

quantification of the expression of the main differentiation-related genes by means of RT-qPCR (Fig. 6). *ALP* and *RUNX-2*, are the most frequently used markers of early osteoblasts/odontogenic differentiation [26]. In the present research, at 3 d time point, cells differentiation was not obtained in any group, except when they were cultured in *OsteoDiff*®; at this medium, cells attained the highest *ALP* expression (Fig. 6A).

As a result, the ALP hydrolization of pyrophosphate into inorganic phosphate as a precursor of mineralization is slowed down [27], regardless of the presence of LPS, in the present research. At 21 d, the presence of NPs, with or without TDg, up-regulated the *ALP* marker even if compared with *OsteoDiff*® (positive control). However, in the presence of LPS the *ALP* expression was down-regulated in both groups, although the differences were less pronounced when TDg was also present. (Fig. 6A). Thereby, it is speculated that Wnt signaling has partially contributed to up-regulate the *ALP* gene expression when TDg-NPs and LPS were both in culture, inducting osteogenic differentiation [6]. The GSK-3β inhibitor (TDg), a Wnt agonist, has demonstrated the capability to induce differentiation of dental pulp cells into odontoblast-like cells [7].

RUNX-2 was over-expressed across all groups at the 21 d compared to the 3 d, without significant differences among the groups (Figs. 6B and 6C). *RUNX-2* is a specific transcription factor that plays a regulatory role in osteoblasts and facilitates osteogenic differentiation of cells [24]. The up-regulation of *RUNX-2* in all groups, when compared with the control group, regardless the presence or not of LPS, suggests the activation of the mitogen-activated protein kinase (MAPK) pathway. This will further enhance cell adhesion and bone matrix formation, even in the presence of a local inflammatory environment (Fig. 6C). *RUNX-2* serves as a master regulator of osteoblast differentiation and it is also known for its role in activating other osteoblastic marker genes [28]. The Wnt transcription factor has been reported to occupy the proximal *RUNX-2* promoter. The binding of the β-catenin to the *RUNX-2* promoter

induces *RUNX-2* expression. Therefore, TDg-mediated Wnt/β-catenin activation stimulated *RUNX-2* transcription [6]. Nevertheless, in presence of inflammatory environment, there is a large amount of nuclear β-catenin that may be sufficient to repress *RUNX2*-dependent activation of osteocalcin promoter in osteoblastic cells, but triggered the β-catenin/lymphoid enhancer binding factor (LEF-1) pathway [21], inhibiting osteogenesis and mineralization, as shown in Figs. 6 and 7. As observed in Fig. 6, there is a tendency toward *RUNX-2* down-regulation in all cultures (OsteoDiff®, NPs, and TDg-NPs) after the addition of LPS, although these differences were not statistically significant. *E. coli*-derived LPS has been shown to reduce *RUNX-2* in scaffold-free dental pulp stem cells constructs [8], suggesting that LPS decreases the odontoblastic differentiation potential of dental pulp stem cells. The referred high presence of β-catenin in the nucleus [21] may have created evident nuclear abnormalities visualized by the F-actin, after analyzing the cytoskeleton by phalloidin staining. Immuno-cytochemical staining with phalloidin evidenced that LPS inclusion in the cultures resulted in cytoskeletal disorganization, lower F-actin fibers content and an aberrant morphology. These features were mitigated cell cultures with TDg. Cells cultured in *OsteoDiff*® and NPs, both with LPS (Figs. 5A and 5B) exhibited multiple diffuse and multifocal blue nuclei, which were condensed and likely related to fragmented nuclei [29], indicating a different actin cytoskeleton organization. It was not produced when doping NPs with TDg, even in presence of LPS (Fig. 5C). These deviations, could be associated with the accumulation of cells in the S phase, affecting the DNA synthesis and altering the biological function of cells [19], as altered actin cytoskeleton plays a role in cellular response to different stimuli [30]. The cytoskeleton, a network of polymeric fibers, is responsible for the integrated cell shape, cell movement, transportation of various molecules, and cell division. Microfilament, microtubule, and intermediate filaments are the types of cytoskeletal elements present in eukaryotic cells [31]. Actin is a microfilament, known for its pivotal role in mitosis, cell survival, and growth by facilitating intracellular and extracellular signaling, apart from maintaining the physical structure of a cell) [32]. It is also known that actin is essentially associated with apoptosis. Apoptosis results in cell destruction caused by a disrupted cytoskeleton, shrunk cells, blebbed cell membranes, condensed nuclei, and fragmented DNA [33]. The presence of LPS has disrupted the normal distribution of microfilaments, especially in the absence of TDg. (Fig. 5C). Incorporation of p38 MAPK activation into the culture medium, in the presence of TDg-NPs and LPS, might enhance osteogenic differentiation and mineralization. The MAPK pathway can activate *RUNX-2*, thereby promoting bone formation [21]. This chance requires further experimentation. Thus, the results of the present study partially support, again, the rejection of the null hypothesis, because there were differences in osteogenic markers expression and morphology of the cytoskeleton in the tested cultures with and without LPS.

RUNX-2 also controls the expression of several genes essential for osteoblastic or odontoblastic differentiation, as *DSPP*, which is required for mineralized tissue formation. *DSPP* is suggested to act as mineralization nucleus for the deposition of the first apatite crystal during the mineralization process [34]. At 21 d time point, *DSPP* gene expression was down-regulated when hDPSCs were cultured in the presence of *OsteoDiff*® and LPS, compared to cultures with *OsteoDiff*® alone (Fig. 6B). Nevertheless, when NPs, with or without TDg, were added to the culture medium, the presence of LPS did not affect *DSPP* gene expression (Fig. 6B). Rothermund *et al.* (2022) [8], stated that LPS reduced the expression of the dentin-related proteins, but in the present research, this reduction only occurred when cells were cultured with *OsteoDiff*®. In the other groups (NPs and TDg-NPS), LPS did not affect *DSPP* gene expression (Fig. 6B).

COL1A1 is one of the most representative components of extracellular matrix found in bone and dentin, being the main constituent of the organic part [34]. *COL1A1* expresses the capacity to synthesize collagen from the human MSCs, which involves differentiation [24]. In the present research, the presence of inflammation (i.e. LPS) revealed significant down-regulation of this gene expression at 21 d time point (Fig. 6D). Therefore, it can be inferred that LPS interferes with collagen synthesis, which is essential for hard tissues remineralization, regardless the presence of TDg.

Studies investigating the effects of LPS on odontogenic differentiation of DPSCs have yielded contradictory results; some reported that LPS did not affect differentiation, while others showed that it either promoted or inhibited DPSCs differentiation [8]. Notably, in the present study, the presence of LPS down-regulated the gene expression of osteonectin at the 21 d time point when cells were cultured with *OsteoDiff*® or NPs. However, this down-regulation was not observed when NPs were doped with TDg (Fig. 6E). This marker serves as an indicator of significant osteoblastic differentiation and mineralization during new bone formation, playing a vital role in bone mineralization, cell-matrix interactions, and collagen binding [35]. Elevated levels of this protein indicate enhanced osteogenic differentiation and accelerated bone matrix mineralization. As a matrix-associated protein, osteonectin promotes mineralization and regulates cellular interactions within the bone matrix [35]. The significant up-regulation of this marker suggests that TDg exerts a potent osteogenic stimulus in presence of LPS, encouraging hDPSCs to differentiation into bone-forming osteoblasts. Furthermore, *ON* serves as a scaffold, binding to hydroxyapatite and other bone proteins to facilitate the integration of minerals and collagen in the bone matrix [36]. This up-regulation may also indicative enhanced intracellular signaling pathways associated with osteogenesis. Elevated levels of osteonectin and other markers suggest the activation of osteoblast-specific genes, resulting in increased osteoblast activity, maturation, and eventual bone formation [35]. This was confirmed by the alizarin red staining technique used in the present research, which revealed multiple precipitated calcium deposits (Fig. 7). The substantial increase in *ON* levels in the presence of TDg-NPs (Fig. 6E) underscores its potential as a promising therapeutic agent for tissue regeneration and repair, even in the case of local inflammation. Given its apparent ability to stimulate key markers of osteogenic differentiation, TDg could be considered for further in vivo studies to validate its efficacy and safety in the context of bone tissue engineering or regenerative medicine. Our findings demonstrate that TDg treatment significantly enhances the expression of important osteogenic markers, such as *ON*, in hDPSCs after 21 d. This suggests that TDg holds promise as a potent inducer of osteogenic differentiation, thereby potentially contributing to bone regeneration and repair strategies. Further research is required to explore the underlying molecular mechanisms and to assess the in vivo effectiveness of TDg in bone regeneration.

Bone sialoprotein (*BSP*), which acts as mineralization nucleus [34] was overexpressed in all groups at 21 d time point, except in the control group (Fig. 6F). This indicates that all osteogenic solutions contributed similarly to the deposition of the first apatite crystals during the mineralization process. In the present study, the amelogenin gene (*AMELX*) was overexpressed when cells were cultured in *OsteoDiff*®, compared to the rest of the groups, which exhibited similar expression levels at the 21 d time point. It is noteworthy that *AMELX* was down-regulated when LPS was added to *OsteoDiff*® (Fig. 6G). *AMELX* is the most representative of the enamel matrix proteins and it also enhances the regeneration of the periodontal tissues [37].

The inflammatory status of the pulp significantly affected the viability and mineralization capacity of the dental pulp stems cells [1,5, 22]. In the present study and in general terms, viability has not been affected at any time point, among the different experimental groups. Only, at 48 h of follow-up, proliferation slightly decreased when cells where cultured with NPs and LPS (Fig. 3). Previous analyses have stated that LPS do not always alter cell viability [1]. Generally, LPS induces inflammatory responses, decreases in cell differentiation of human DPCs, impairment of mitochondrial dynamics and increases at the levels of antioxidants without interfering with apoptosis and cell proliferation [4,5,22]. Earlier studies have even shown increased cell proliferation at

0.5–1 μg/mL of LPS, meanwhile inconsistent data have been obtained at higher concentrations [38]. Other authors [4] did not attain any differences in human DPCs proliferation treated with 20 μg/mL of LPS at day 1, 3 and 7, and others neither obtained significant differences in cell proliferation in presence of TDg [6]. Nevertheless, Tabassum *et al.* (2023) [7] obtained odontoblast proliferation at 3 d after loading a polymeric scaffold with TDg when determining the gene expression of *ALP* and *DSPP*. It is speculated that, probably, the different carrier, the dissimilar kinetic release and distinct methodology make the results to be different.

To determine the impact on cell migration, it was decided to use wound healing assays, in order to predict how the coordinated migration of hDPSCs would occur during inflammation, or after wound infliction measuring the delay or improvement of healing [39]. When odontoblasts dye, they are replaced by odontoblasts-like cells differentiated out of stem cells located in the pulp, which migrate to the destruction site and participate in the healing process of the tissue) [1]. Nevertheless, cell migration in the present study was not affected by the presence of TDg and/or LPS, but was progressively increasing over time (Fig. 4). Li *et al.* (2014) [2] showed the effect of LPS increasing the migration of DPSCs. They used determination of some chemotactic factors to assess migration. However, previous reports have demonstrated that TDg impaired the proliferation and migration of several cancer cell types, probing that Wnt signaling is cell type specific [6]. The evidence highlights that the use of different in vitro models (i.e, different cell cultures, types of culture media, different compositions and concentrations or biomaterial exposure times) precludes a meaningful comparison of the results reported in those studies [40].

To the authors' knowledge, this is the first study to describe the biological response of hDPSCs to polymeric nanoparticles doped with TDg in the presence of LPS. This research has shown several shortcomings and limitations. It is an in vitro study which might not totally represent the responses that occur in vivo. The lack of NPs characterization should be considered as a limitation of the present research. However, the NPs have been widely characterized in previous investigations [41–43] and it has been shown that the hydrodynamic size distribution of NPs, assessed by dynamic light scattering, does not change after loading and no agglomeration is produced. If explored by FTIR, the spectra have the same number of bands because the binding of drugs did not provide new functional groups that might give rise to different vibrational modes. Transmission and scanning electron microscopy morphological images of NPs also remained similar before and after doping. Otherwise, TDg liberation was not measured because NPs are non-resorbable and TDg may be acting on cells even when it is not being released by NPs.

Further research on mechanistic studies is needed to evaluate the exact mode of action controlling the activity of the novel material investigated in this work. LPS is a component of the external membrane of gram-negative bacteria. A combination of LPS and H_2O_2 should also be interesting to investigate, as this blend represents the most effective way of inducing pulpal injury, resulting in pulpitis, since LPS and H_2O_2 often occurs together during clinical pulpitis [4]. Experiments performed in animal models could be complementary to the present in vitro study, in order to investigate the pulpal regeneration ability of the present TDg-NPs. In addition, candidate genes from RNA sequencing and bioinformatics analysis could be selected and gene silencing could be used to investigate the effect on hDPSCs odonto/osteogenic differentiation. Our results should act as preliminary evidence for the development of future actions on different cell lines, animal models, and/or clinical trials.

5. Conclusions

LPS in the cell cultures induced lower mineral deposition; however, tideglusib-doped nanoparticles (TDg-NPs) effectively mitigated this effect, promoting regenerative mineralization even in the presence of LPS. Immunocytochemical staining with phalloidin revealed that LPS led to reduced F-actin fiber content and cytoskeletal disorganization, but these adverse effects were counteracted by TDg-NPs.

These findings suggest that TDg-NPs could be a promising strategy for enhancing the osteogenic potential of hDPSCs in bone tissue engineering and regenerative medicine.

Declaration of Competing Interest

The authors declare that they have no conflict of interest.

Acknowledgements

This research has been supported by the Spanish Ministry of Science and Innovation MCIN/AEI 10.13039/501100011033 [Grant numbers PID2020–114694RB-I00, PID2020–115887GB-I00].

References

[1] Bucchi C, Bucchi A, Martínez-Rodríguez P. Biological properties of dental pulp stem cells isolated from inflamed and healthy pulp and cultured in an inflammatory microenvironment. J Endod 2023;49(4):395–401.e6. https://doi.org/10.1016/j.joen.2023.02.002.
[2] Li D, Fu L, Zhang Y, Yu Q, Ma F, Wang Z, Luo Z, Zhou Z, Cooper PR, He W. The effects of LPS on adhesion and migration of human dental pulp stem cells in vitro. J Dent 2014;42(10):1327–34. https://doi.org/10.1016/j.jdent.2014.07.007.
[3] Kishimoto T, Kaneko T, Ukai T, Yokoyama M, Ayon Haro R, Yoshinaga Y, Yoshimura A, Hara Y. Peptidoglycan and lipopolysaccharide synergistically enhance bone resorption and osteoclastogenesis. J Periodontal Res 2012;47(4):446–54. https://doi.org/10.1111/j.1600-0765.2011.01452.x.
[4] Vaseenon S, Srisuwan T, Chattipakorn N, Chattipakorn SC. Lipopolysaccharides and hydrogen peroxide induce contrasting pathological conditions in dental pulpal cells. Int Endod J 2023;56(2):179–92. https://doi.org/10.1111/iej.13853.
[5] Brodzikowska A, Ciechanowska M, Kopka M, Stachura A, Włodarski PK. Role of lipopolysaccharide, derived from various bacterial species, in pulpitis- a systematic review. Biomolecules 2022;12(1):138. https://doi.org/10.3390/biom12010138.
[6] Kornsuthisopon C, Tompkins KA, Osathanon T. Tideglusib enhances odontogenic differentiation in human dental pulp stem cells in vitro. Int Endod J 2023;56(3):369–84. https://doi.org/10.1111/iej.13877.
[7] Tabassum N, Khalid S, Ghafoor S, Woo KM, Lee EH, Samie M, Konain K, Ponnusamy S, Arany P, Rahman SU. Tideglusib-incorporated nanofibrous scaffolds potently induce odontogenic differentiation. J Biomater Appl 2023;38(2):280–91. https://doi.org/10.1177/08853282231190470.
[8] Rothermund K, Calabrese TC, Syed-Picard FN. Differential effects of escherichia coli- versus porphyromonas gingivalis-derived lipopolysaccharides on dental pulp stem cell differentiation in scaffold-free engineered tissues. J Endod 2022;48(11):1378–1386.e2. https://doi.org/10.1016/j.joen.2022.08.010.
[9] Wang C, Liao H, Cao Z. Role of osterix and MicroRNAs in bone formation and tooth development. Med Sci Monit 2016;22:2934–42. https://doi.org/10.12659/msm.896742.
[10] Nemoto E, Koshikawa Y, Kanaya S, Tsuchiya M, Tamura M, Somerman MJ, Shimauchi H. Wnt signaling inhibits cementoblast differentiation and promotes proliferation. Bone 2009;44(5):805–12. https://doi.org/10.1016/j.bone.2008.12.029.
[11] Takahashi-Yanaga F. Activator or inhibitor? GSK-3 as a new drug target. Biochem Pharm 2013;86(2):191–9. https://doi.org/10.1016/j.bcp.2013.04.022.
[12] Pandey MK, DeGrado TR. Glycogen Synthase Kinase-3 (GSK-3)-targeted therapy and imaging. Theranostics 2016;6(4):571–93. https://doi.org/10.7150/thno.14334.
[13] Lovestone S, Boada M, Dubois B, Hüll M, Rinne JO, Huppertz HJ, Calero M, Andrés MV, Gómez-Carrillo B, León T, del Ser T. ARGO investigators. A phase II trial of tideglusib in Alzheimer's disease. J Alzheimers Dis 2015;45(1):75–88. https://doi.org/10.3233/JAD-141959.
[14] Toledano M, Fernández-Romero E, Aguilera FS, Osorio E, Rodríguez-Santana JA, Garrido M, Solís PA, García-Godoy F, Osorio R. Tunable polymer-peptide hybrids for dentin tissue repair. J Dent 2024:105027. https://doi.org/10.1016/j.jdent.2024.105027.
[15] Toledano M, Aguilera FS, Fernández-Romero E, Lagos AJ, Bonilla M, Lynch CD, Osorio R. Dentin remineralization using a stimuli-responsive engineered small molecule GSK3 antagonists-functionalized adhesive. Dent Mater 2024;40(3):393–406. https://doi.org/10.1016/j.dental.2023.12.010.
[16] Medina-Castillo AL. Thermodynamic principles of precipitation polymerization and role of fractal nanostructures in the particle size control. Macromolecules 2020;53(14):5687–700. https://doi.org/10.1021/acs.macromol.0c00973.
[17] García-Bernal D, López-García S, Sanz JL, Guerrero-Gironés J, García-Navarro EM, Moraleda JM, Forner L, Rodríguez-Lozano FJ. Melatonin treatment alters biological and immunomodulatory properties of human dental pulp mesenchymal stem cells via augmented transforming growth factor beta secretion. J Endod 2021;47(3):424–35. https://doi.org/10.1016/j.joen.2020.12.008.

[18] Toledano-Osorio M, de Luna-Bertos E, Toledano M, Manzano-Moreno FJ, Ruiz C, Sanz M, Osorio R. NP-12 peptide functionalized nanoparticles counteract the effect of bacterial lipopolysaccharide on cultured osteoblasts. 00159-3 Dent Mater 2024; S0109-5641(24). https://doi.org/10.1016/j.dental.2024.06.017.
[19] Toledano-Osorio M, López-García S, Osorio R, Toledano M, García-Bernal D, Sánchez-Bautista S, Rodríguez-Lozano FJ. Dexamethasone and doxycycline doped nanoparticles increase the differentiation potential of human bone marrow stem cells. Pharmaceutics 2022;14:1865. https://doi.org/10.3390/pharmaceutics14091865.
[20] Rodríguez-Lozano FJ, Collado-González M, Tomás-Catalá CJ, García-Bernal D, López S, Oñate-Sánchez RE, Moraleda JM, Murcia L. GuttaFlow Bioseal promotes spontaneous differentiation of human periodontal ligament stem cells into cementoblast-like cells. Dent Mater 2019;35(1):114–24. https://doi.org/10.1016/j.dental.2018.11.003.
[21] Liu N, Shi S, Deng M, Tang L, Zhang G, Liu N, Ding B, Liu W, Liu Y, Shi H, Liu L, Jin Y. High levels of β-catenin signaling reduce osteogenic differentiation of stem cells in inflammatory microenvironments through inhibition of the noncanonical Wnt pathway. J Bone Min Res 2011;26(9):2082–95. https://doi.org/10.1002/jbmr.440.
[22] Noori MS, Courreges MC, Bergmeier SC, McCall KD, Goetz DJ. Modulation of LPS-induced inflammatory cytokine production by a novel glycogen synthase kinase-3 inhibitor. Eur J Pharm 2020;883:173340. https://doi.org/10.1016/j.ejphar.2020.173340.
[23] Hara M, Horibe K, Mori H, Nakamura H. The role of canonical Wnt signaling in dentin bridge formation. J Oral Biosci 2021;63(2):199–209. https://doi.org/10.1016/j.job.2021.03.003.
[24] Li Y, Wu M, Xing X, Li X, Shi C. Effect of Wnt10a/β-catenin signaling pathway on promoting the repair of different types of dentin-pulp injury. Vitr Cell Dev Biol Anim 2023;59(7):486–504. https://doi.org/10.1007/s11626-023-00785-z.
[25] Florimond M, Minic S, Sharpe P, Chaussain C, Renard E, Boukpessi T. Modulators of Wnt signaling pathway implied in dentin pulp complex engineering: a literature review. Int J Mol Sci 2022;23(18):10582. https://doi.org/10.3390/ijms231810582.
[26] Li Y, Huang X, Fu W, Zhang Z, Xiao K, Lv H. Preparation of PDA-GO/CS composite scaffold and its effects on the biological properties of human dental pulp stem cells. BMC Oral Health 2024;24(1):157. https://doi.org/10.1186/s12903-023-03849-4.
[27] Orriss IR, Arnett TR, Russell RG. Pyrophosphate: a key inhibitor of mineralisation. Curr Opin Pharm 2016;28:57–68. https://doi.org/10.1016/j.coph.2016.03.003.
[28] Suzuki N, Hanmoto T, Yano S, Furusawa Y, Ikegame M, Tabuchi Y, Kondo T, Kitamura K, Endo M, Yamamoto T, Sekiguchi T, Urata M, Mikuni-Takagaki Y, Hattori A. Low-intensity pulsed ultrasound induces apoptosis in osteoclasts: Fish scales are a suitable model for the analysis of bone metabolism by ultrasound. Comp Biochem Physiol A Mol Integr Physiol 2016;195:26–31. https://doi.org/10.1016/j.cbpa.2016.01.022.
[29] Mohamed Azar KAH, Ezhilarasan D, Shree Harini K. Coleus vettiveroides ethanolic root extract induces cytotoxicity by intrinsic apoptosis in HepG2 cells. J Appl Toxicol 2024;44(2):245–59. https://doi.org/10.1002/jat.4536.
[30] Acevedo K, Moussi N, Li R, Soo P, Bernard O. LIM kinase 2 is widely expressed in all tissues. J Histochem Cytochem 2006;54(5):487–501. https://doi.org/10.1369/jhc.5C6813.2006.
[31] Tang DD, Gerlach BD. The roles and regulation of the actin cytoskeleton, intermediate filaments and microtubules in smooth muscle cell migration. Respir Res 2017;18(1):54. https://doi.org/10.1186/s12931-017-0544-7.
[32] Prasain N, Stevens T. The actin cytoskeleton in endothelial cell phenotypes. Micro Res 2009;77(1):53–63. https://doi.org/10.1016/j.mvr.2008.09.012.
[33] Harada H, Grant S. Apoptosis regulators. Rev Clin Exp Hematol 2003;7(2):117–38.
[34] Hunter GK, Goldberg HA. Modulation of crystal formation by bone phosphoproteins: role of glutamic acid-rich sequences in the nucleation of hydroxyapatite by bone sialoprotein. Biochem J 1994;302(1):175–9.
[35] Vimalraj S, Govindarajan D, Sudhakar S, Suresh R, Palanivel P, Sekaran S. Chitosan derived chito-oligosaccharides promote osteoblast differentiation and offer anti-osteoporotic potential: Molecular and morphological evidence from a zebrafish model. Int J Biol Macromol 2024;259(Pt 2)):129250. https://doi.org/10.1016/j.ijbiomac.2024.129250.
[36] Mansour A, Mezour MA, Badran Z, Tamimi F *. Extracellular matrices for bone regeneration: a literature review. Tissue Eng Part A 2017;23(23-24):1436–51. https://doi.org/10.1089/ten.TEA.2017.0026.
[37] Nibali L, Koidou VP, Nieri M, Barbato L, Pagliaro U, Cairo F. Regenerative surgery versus access flap for the treatment of intra-bony periodontal defects: A systematic review and meta-analysis. J Clin Periodo 2020;47(Suppl 22):320–51. https://doi.org/10.1111/jcpe.13237.
[38] Lei S, Liu XM, Liu Y, Bi J, Zhu S, Chen X. Lipopolysaccharide downregulates the osteo-/odontogenic differentiation of stem cells from apical papilla by inducing autophagy. J Endod 2020;46(4):502–8. https://doi.org/10.1016/j.joen.2020.01.009.
[39] López-García S, Pecci-Lloret MP, Pecci-Lloret MR, Guerrero-Gironés J, Rodríguez-Lozano FJ, García-Bernal D. Topical fluoride varnishes promote several biological responses on human gingival cells. Ann Anat 2021;237:151723. https://doi.org/10.1016/j.aanat.2021.151723.
[40] Peters OA. Research that matters - biocompatibility and cytotoxicity screening. Int Endod J 2013;46(3):195–7. https://doi.org/10.1111/iej.12047.
[41] Toledano-Osorio M, Osorio E, Aguilera FS, Luis Medina-Castillo A, Toledano M, Osorio R. Improved reactive nanoparticles to treat dentin hypersensitivity. Acta Biomater 2018;72:371–80. https://doi.org/10.1016/j.actbio.2018.03.033.
[42] Toledano M, Osorio E, Osorio MT, Aguilera FS, Toledano R, Romero EF, Osorio R. Dexamethasone-doped nanoparticles improve mineralization, crystallinity and collagen structure of human dentin. J Dent 2023;130:104447. https://doi.org/10.1016/j.jdent.2023.104447.
[43] Osorio MT, Toledano R, Huang H, Toledano-Osorio M, Osorio R, Huang CC, García-Godoy F. Effect of doxycycline doped nanoparticles on osteogenic/cementogenic and anti-inflammatory responses of human cells derived from the periodontal ligament. J Dent 2023;137:104668. https://doi.org/10.1016/j.jdent.2023.104668.